

Fatigue Damage Accumulation in a Cu-based Shape Memory Alloy: Preliminary Investigation

F. Casciati¹, S. Casciati², L. Faravelli¹ and A. Marzi¹

Abstract: The potential offered by the main features of shape memory alloys (SMA) in Structural Engineering applications is object of attention since two decades. The main issues concern the predictability of the material behavior and the fatigue lifetime of macro structural elements (as different from wire segments). In this paper, the fatigue characteristics, at given temperatures, of multigrain samples of a specific Cu-based alloy are investigated. The results of laboratory tests on bar specimens are discussed. The target is to model the manner in which the effects of several loading-unloading cycles of different amplitude cumulate.

Keywords: Damage accumulation, Fatigue, Shape memory alloy, Training.

1 Introduction

The potential offered by the main features of shape memory alloys (SMA) in Structural Engineering applications is the object of scientific and technical attention since more than two decades [Graesser-Cozzarelli, 1991; Dolce et al., 2000; Ip, 2000; Des Roches et al., 2004; Casciati-Faravelli, 2008; Casciati-van der Eijk, 2008; Casciati-Faravelli, 2009; Saiidi et al., 2009]. In these studies, macrostructural (multi grains) elements are considered and it is difficult to extend to them the large amount of physical investigations and numerical modeling developed in literature for single crystal samples (see, for instance, [Meunier et al., 1996] as an early reference).

Some fatigue studies for the classic Ni-Ti alloy were recently published [Nemat Nasser-Guo, 2006; Roy et al., 2008; Zhang et al., 2008; Bertacchini et al., 2009]. Studies of the fatigue behavior of single-grain Copper-based SMA are also available in literature [Siredey-Eberhardt, 2000; Siredey et al. 2005].

In this paper, the fatigue characteristics, at given temperatures, of multigrain samples of a specific Cu-based alloy are investigated. The main issues concern the

¹ University of Pavia, Pavia, Italy

² University of Catania, Siracusa, Italy, saracasciati@msn.com

predictability of the material behavior [Carreras et al., 2011] and the fatigue lifetime [Casciati et al., 2008; Casciati-Marzi, 2010, Faravelli-Marzi, 2010, Casciati-Marzi, 2011]. In the previous works, laboratory tests were carried out by applying loading-unloading cycles of constant amplitude. To provide further insight on the studied phenomenon, the target of modeling the manner in which the effects of several cycles of different amplitude cumulate is herein pursued. In particular, the original contribution of the present paper consists of laying the basis to model the accumulation of fatigue damage in the specific Cu-based SMA with superelastic behavior under consideration. For this purpose, a preliminary investigation of the damage accumulation phenomenon is carried out by setting up a properly targeted experimental campaign. The data achieved from the laboratory tests are then used to verify the validity of the classical Miner's damage accumulation rule. Furthermore, the possibility of an early alert of fatigue collapse is investigated by tracking the variation of a dimensionless parameter associated with the energy dissipated per cycle and calculated from the measurements of strain gauges and load cells. Finally, a trigger for the replacement of the monitored SMA macro-structural element is proposed so that a satisfactory percentage of its actual fatigue lifetime is exploited in the maintenance policy.

2 Governing relations

The specific alloy studied in this contribution has chemical composition 87.7% Cu - 11.8% Al - 0.5% Be, where the percentages express the relative weights of the components. The alloy is cast in ingots which are then transformed into suitable structural elements such as wires, bars or plates. The phase transformations temperatures are given as follows: martensite starts at -46°C ; martensite finishes at -55°C ; austenite starts at -25°C ; austenite finishes at -18°C . These values can be altered by applying thermal treatments to the SMA specimens, but, in general, the alloy shows a superelastic behavior at any positive value of temperature, with the hysteresis cycles progressively shrinking as the temperature increases. For this reason, such an alloy is considered as suitable to the realization of passive devices for the mitigation of vibrations in Civil Engineering structures. Furthermore, in contrast to NiTi alloy, its fabrication does not require any void processing, thus leading to a lower cost on the market.

When a mechanical test consisting of a low number of loading-unloading cycles is performed on the specimen at its early stage of production, a deterioration of the hysteretic diagram is observed as the loading-unloading cycles are repeated at any given temperature in the range from 10°C to 80°C [Casciati-van der Eijk, 2008; Casciati-Faravelli, 2009]. Indeed, the residual martensite retained in the specimen by micro-plasticity during the cyclic loading induces residual strain at the end of the

unloading and results in a reduction of the hysteretic loop area. This inconvenience is overcome by preliminarily applying to the specimen a suitable thermal treatment, so that the stabilization of the material behavior is achieved.

The following general expression, valid for any material, can be used to model the stress-strain relationship describing each loading-unloading cycle of a mono-axial tension test carried out on a SMA specimen in a controlled thermal environment:

$$\sigma(t) = \sigma(\varepsilon(t), \varepsilon_{\max}, \varepsilon_{\min}, \sigma_{\max}, \sigma_{\min}, \eta | \Theta, \Gamma, f_c) \tag{1}$$

where $\sigma(t)$ is the stress at time t ;

$\varepsilon(t)$ is the strain at time t ;

$\varepsilon_{\max}, \varepsilon_{\min}$ are the strain maximum and minimum values during the cycle, respectively;

$\sigma_{\max}, \sigma_{\min}$ are the stress maximum and minimum values during the cycle, respectively;

η is a dimensionless parameter indicating the size of the hysteresis loop;

Θ is the temperature of the controlled environment;

Γ is a linguistic label used to specify the thermal treatment undergone by the specimen;

f_c is the frequency of the cycles.

The definition of the parameter η in Eq. (1) requires to introduce the energy dissipated per cycle which is given by

$$\mathfrak{S}_c = \oint P du = \oint \sigma A d\varepsilon L_0 = V_0 \oint \sigma d\varepsilon \tag{2}$$

where A and L_0 denote the cross section area and the initial length of the specimen, respectively, P the tension load, and u the specimen elongation which coincides with the span of the testing machine. In the stress-strain plane, let $P \equiv (\varepsilon_{\min}, \sigma_{\min})$ and $Q \equiv (\varepsilon_{\max}, \sigma_{\max})$ the geometrical points denoting the edges of the hysteretic cycle. The distance between these two points is measured using the Pythagorean metrics and it is denoted as $d = \overline{PQ}$. If a single stress-strain cycle is approximated by an inclined ellipse of diameters d and ηd , with d given by:

$$d = \sqrt{a(\varepsilon_{\max} - \varepsilon_{\min})^2 + b(\sigma_{\max} - \sigma_{\min})^2} \approx |\sigma_{\max} - \sigma_{\min}| \tag{3}$$

where $a = 1 \text{ MPa}$ and $b = 1 \text{ MPa}^{-1}$ are the unit conversion factors, then the energy per cycle per unit volume can be written as:

$$\mathfrak{S}_c/V_0 = \pi \eta d^2/4 \tag{4}$$

Lastly, Eq. (4) is used to assess the value of η . During a fatigue test characterized by a high number of cycle, the subsequent values assumed by this parameter are useful to quantify the degradation of the hysteretic loop, which is due to the changes in phase of the alloy components. Once again this phenomenon is a consequence of the residual martensite retained in the specimen by micro-plasticity during the cyclic loading. The change in phase occurrence is also made evident by the reduction of the stress level at which the constant deformation plateau is reached. Such a remark suggests that the fatigue tests should not be carried out in load control, because it would require to assign the maximum value of stress during each cycle. By contrast, two different approaches can be pursued:

- span control between the given maximum and minimum values of the strain. Each corresponding loading-unloading cycle would then be modeled by a relationship of the type:

$$\sigma(t) = \sigma(\varepsilon(t), \sigma_{\max}, \sigma_{\min}, \eta | \Theta, \Gamma, f_c, \varepsilon_{\max}, \varepsilon_{\min}) \quad (5)$$

- span control from zero load to the assigned maximum strain value and load control for the unloading to zero. Each corresponding loading-unloading cycle would then be modeled by a relationship of the type:

$$\sigma(t) = \sigma(\varepsilon(t), \varepsilon_{\min}, \sigma_{\max}, \eta | \Theta, \Gamma, f_c, \varepsilon_{\max}, \sigma_{\min}) \quad (6)$$

In each case, the unassigned parameters ($\sigma_{\max}, \sigma_{\min}$ or $\sigma_{\max}, \varepsilon_{\min}$) are recorded during the test and their time histories can be used to characterize the degradation of the hysteretic loop.

3 Fatigue tests

The fatigue tests reported in this paper were conducted in span control during the loading and in load control during the unloading (case b, in the previous section). Therefore, the minimum strain value ε_{\min} and the maximum stress value σ_{\max} are the a priori unknown parameters which need to be recorded at the beginning and at the end of the loading step of the current cycle, respectively. It is worth noticing that ε_{\min} also represents the residual strain value at the end of the previous cycle. In the following, the graphical representation of the results from the fatigue tests include the recorded time histories of this quantity (as shown, for instance, in Figure 1b).

The fatigue tests were carried out on bars of diameter 3.5 mm at temperatures of 25 °C and 50°C, which represent the typical temperature value of a standard inside working environment and the outside thermal condition when direct exposition to the sun is considered, respectively.

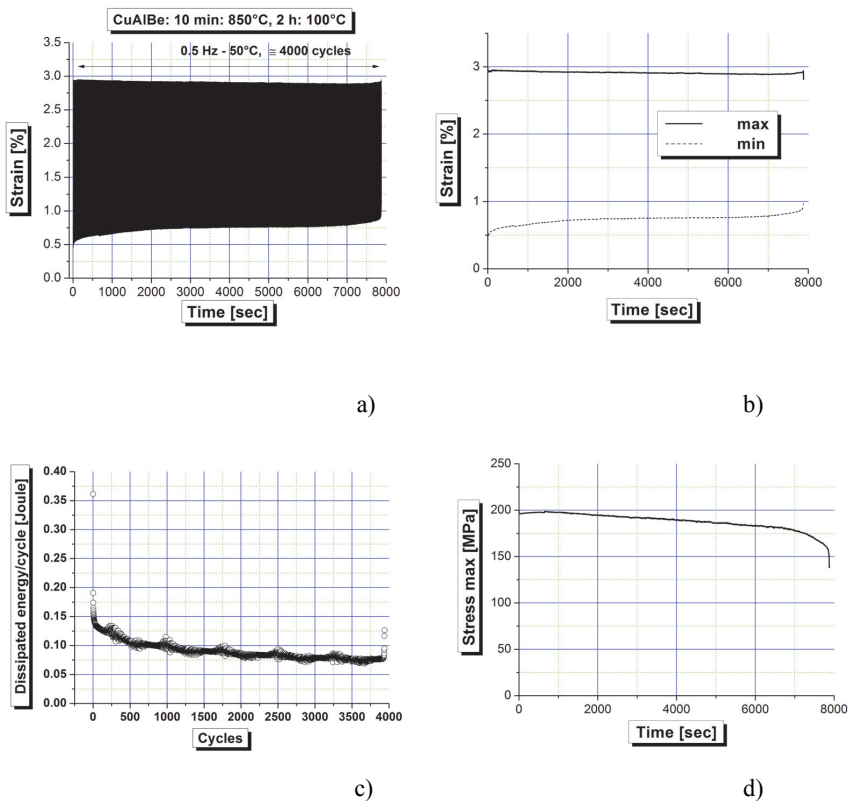


Figure 1: Results from the fatigue test with no preliminary mechanical treatment and cycles up to 3% of strain and down to zero load at temperature $\Theta = 50^{\circ}\text{C}$: (a) strain time history; (b) details of the time histories of the maximum and minimum values of strain; (c) time history of the dissipated energy per cycle; and (d) time history of the maximum stress.

A series of standard fatigue tests are carried out with cycles of constant amplitude. For sake of exemplification, the results in Figure 1 are obtained from a test at temperature $\Theta=50^{\circ}\text{C}$, with no preliminary mechanical treatments, frequency of 0.5 Hz, and maximum value of strain in the cycle of 3%. The initial thermal treatment consisted of 10 minutes at 850°C, fast quenching in water at ambient temperature, and finally 2 hours at 100°C.

It is worth noticing that the assigned maximum strain value of 3% is associated to a

volume fraction of martensite, which can directly be estimated by taking resistivity measurements during the test [Casciati-Rossi, 2006]. Nevertheless, this aspect is beyond the scope of the present study. Additional tests with values of maximum strain higher and lower than 3% (i.e., corresponding to higher and lower values of induced volume fraction of martensite) were conducted in preliminary studies [Casciati-Marzi, 2010] whose outcomes induced the author to identify a maximum strain value in the range of 2-3% as suitable for further investigations of the fatigue damage accumulation, which is the topic of the present paper. Indeed, values of maximum strain below this range do not enable to observe the specific superelastic feature of SMA materials, whereas values greater than 3% could lead to a premature rupture of the specimen. For 3% of strain, the volume fraction of martensite is very high and the cyclic loading should induce a high decrease of the maximum strain value for a very low number of cycles, if the test was carried out in load control. Nevertheless, this phenomenon is not observed when the test is conducted in span control, being the maximum strain value a priori fixed in the test setup.

The aim of the plots in Figure 1 is to distinguish the loss of specific properties of SMA during the cyclic loading from the fatigue effect related to the classical damage observed in a wide range of metallic materials. In particular, the upward trend of the minimum strain time history in Figure 1b is related to the progressive increase of the retained martensite volume fraction in the specimen as the test proceeds, because it represents the accumulation of residual strain. As a consequence, the excursion of each successive cycle shortens, thus altering the shape of the hysteresis loop. Hence, the area within the loop progressively shrinks and the area reduction is proportional to the energy dissipated per cycle, whose time history consistently decreases as shown in the plot of Figure 1c. Finally, these observations are confirmed also by the descendent trend of the maximum stress time history plotted in Figure 1d. This behavior corresponds to a decrease of the maximum transformation strain. Its short initial increase is due to the heating of the specimen during the cyclic loading which causes a shift of the transformation temperatures.

The maximum number of cycles up to when failure occurs is recorded equal to 4000 for the test in Figure 1. From Figures 1b and 1d, it can be observed that the rupture of the specimen follows almost immediately a sudden loss of rigidity. Therefore, the number of cycles required for the loss of rigidity to become evident nearly coincides with the one recorded at the end of the test.

In Figure 2, the time history of the dimensionless parameter η defined in Eq.(4) is drawn and it shows a regular trend to failure.

Recently, in [Carreras et al., 2011], a preliminary mechanical treatment was introduced to enhance the material properties. It consists of two sequences of sets of

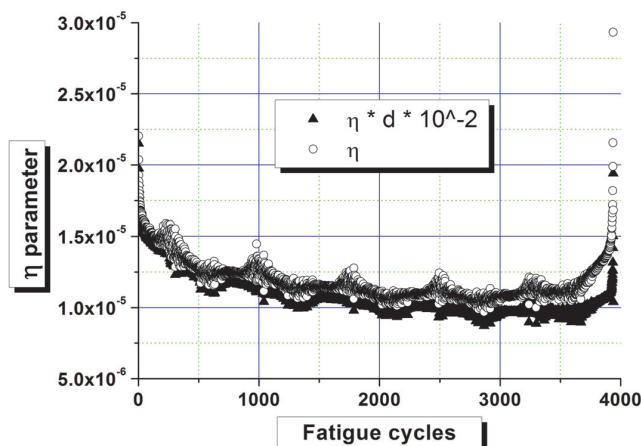


Figure 2: Time histories of the parameter η and of the elliptic cycle radius ηd .

a low number of cycles, with a maximum value of strain which progressively increases from one set to the next one in the same sequence. The final maximum strain value reached in the last set of cycles of the second sequence is then used to set the constant amplitude of the actual fatigue test which ends with the rupture of the specimen. The first sequence of the mechanical treatment is characterized by a temperature which is higher than the one adopted for the rest of the test. Figure 3 is herein inserted for a mere illustrative purpose. It refers to an alloy of the same composition of the one discussed in the present paper and such an alloy presents a superelastic behavior at any positive temperature. Nevertheless, the tested specimen underwent a different initial thermal treatment consisting of 10 minutes at 850°C, fast quenching in water at ambient temperature, and finally one week at 100°C. Furthermore, the fatigue test in Figure 3 is performed at $\Theta=25^\circ\text{C}$ with cycles up to 5.5%, which is a value of maximum strain that falls beyond the above defined working interval of 2-3%. Within the context of the present paper, the interest in the plot of Figure 3 is, therefore, targeted to emphasize that fatigue tests were also carried out at higher maximum strain levels and that different preliminary thermo-mechanical treatments were studied. In particular, a similar preliminary mechanical treatment consisting of only the second sequence of sets of low number of cycles is performed also in the tests discussed in the next Section. The reader interested in further details on the fatigue response of the material at high values of maximum strain is addressed to [Carreras et al., 2011].

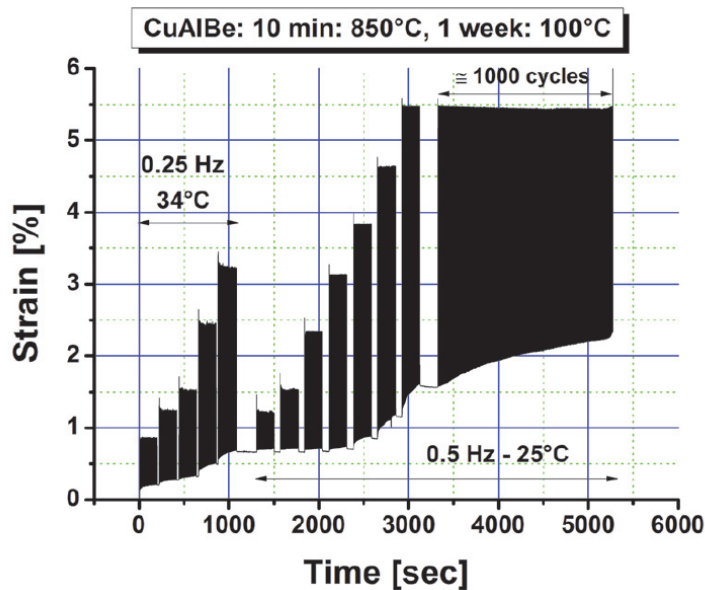


Figure 3: Preliminary mechanical treatment for a fatigue test at $\Theta = 25^{\circ}\text{C}$ with cycles up to 5.5% of strain and down to zero load.

4 Damage accumulation

The original contribution of the present paper consists of laying the basis to model the accumulation of fatigue damage in the specific Cu-based SMA with superelastic behavior under consideration. For this purpose, a preliminary investigation of the damage accumulation phenomenon is carried out by setting up a properly targeted experimental campaign. Three specimens of diameter 3.5 mm obtained from the same ingot of Cu-based alloy with the above defined composition are tested. All three of them were preliminarily subjected to both the following physical processes:

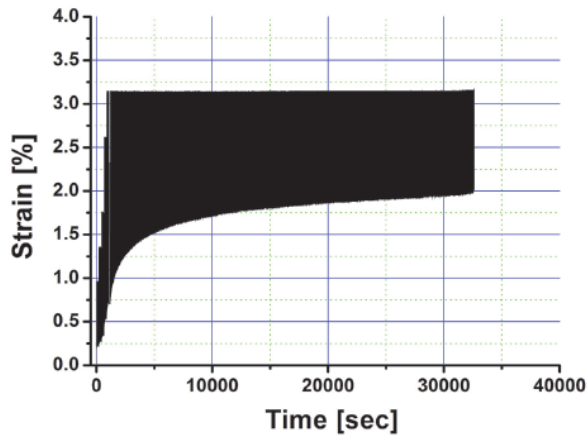
- a thermal treatment consisting of 10 minutes at 850°C , fast quenching in water at ambient temperature, and finally 2 hours at 100°C ;
- a mechanical treatment consisting of a sequence of five successive sets of 50 cycles, each carried out at $\Theta=25^{\circ}\text{C}$ with a frequency of 0.25 Hz. Each set is characterized by a different maximum value of strain in the cycle, being this value assigned so that it progressively increases from one set to the next one; namely, the given values of maximum strain are 0.9%, 1.3%, 1.75%, 2.6% and 3.15%, respectively.

Each specimen is used to undergo a fatigue test characterized by a different definition of the cycles amplitude. In contrast to the fatigue test in Figure 3, the ones herein presented do not necessarily assume as maximum strain the value reached in the last set of cycles during the preliminary mechanical treatment. Furthermore, whereas, in the tests labeled as 1 and 2, cycles of constant amplitude corresponding to a maximum strain value equal to 3.2% and 2.3%, respectively, are identically repeated until rupture, in the test labeled as 3 the rupture is reached by repeatedly performing a sequence where the first 1000 cycles up to 2.3% are followed by other 1000 cycles up to 3.2%. It is worth noting that no general conclusion can be achieved on the basis of only one fatigue test for each loading case, since the fatigue behavior generally presents a high scattering level. Nevertheless, the presence of uncertainties is taken into account by the damage accumulation models discussed in the next Section.

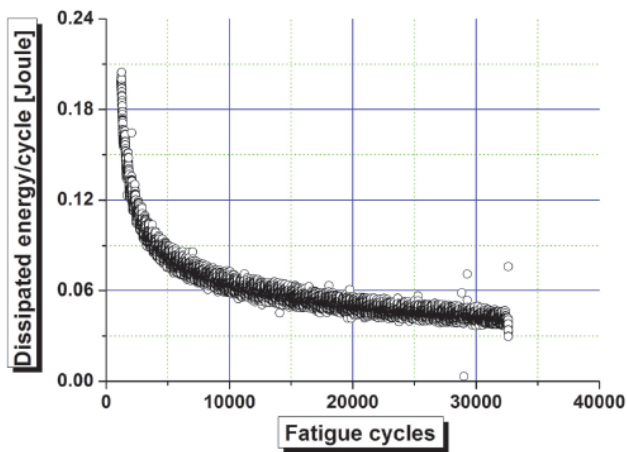
All three tests are carried out at $\Theta=25^{\circ}\text{C}$ with a frequency of 1 cycle per second. The selection of such a frequency value is based on the experience gathered during the experimental campaign reported in [Casciati-Marzi 2010] and it is motivated by the need of compromising between a speed sufficiently low to capture the desired superelastic behavior and sufficiently high to perform the number of cycles required to investigate the fatigue phenomenon in a reasonable time. In general, it is important to evaluate the frequency effect because the SMA behavior is highly sensitive to temperature and there is a little heating induced by dynamic loading, which can have strong consequences on the phase transformation and on the global thermo-mechanical behavior.

The graphical representation of the results is conducted accordingly to what has been done in Figures 1 and 2 of the previous Section for a fatigue test without preliminary mechanical treatment. For sake of conciseness, however, only the time histories of the strain, the energy dissipated per cycle, and the dimensionless parameter η are herein reported. To each of these quantities is dedicated a plot which can be found in Figures 4a, 4b, and 5 for test 1, in Figures 6a, 6b, and 7 for test 2, and in Figures 8a, 9b, and 10a for test 3, respectively. In Figure 8b, the evolution of the load during test 3 is also provided.

From Figure 4a, the maximum number of cycles up to failure in test 1 is equal to 32620 and it is one order of magnitude greater than the one read from Figure 1 in the previous Section. Indeed, this result is obtained at an ambient temperature (25°C) lower than the 50°C of Figure 1 and with a maximum strain (3.2%) which is only slightly greater than the 3% of Figure 1. For test 2, a further increase up to 80413 cycles is reported in Figure 6a and it is achieved by dropping the assigned value of maximum strain in each cycle to 2.3%. An intermediate value of 39654 cycles is obtained for test 3 in Figure 8.



a)



b)

Figure 4: Fatigue test with preliminary mechanical treatment and then cycles up to 3.2% of strain and down to zero load. $\Theta = 25^{\circ}\text{C}$. a) full test with emphasis on the increasing of the residual strain; b) dissipated energy per cycle.

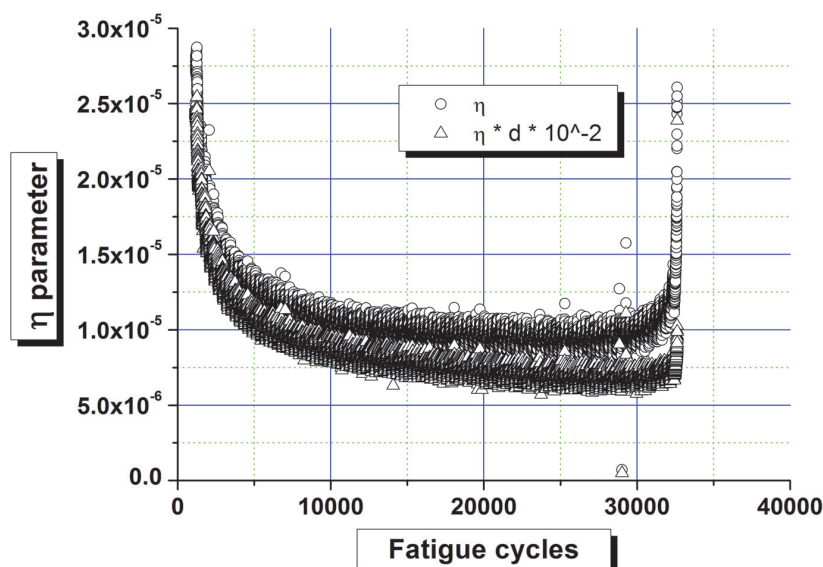
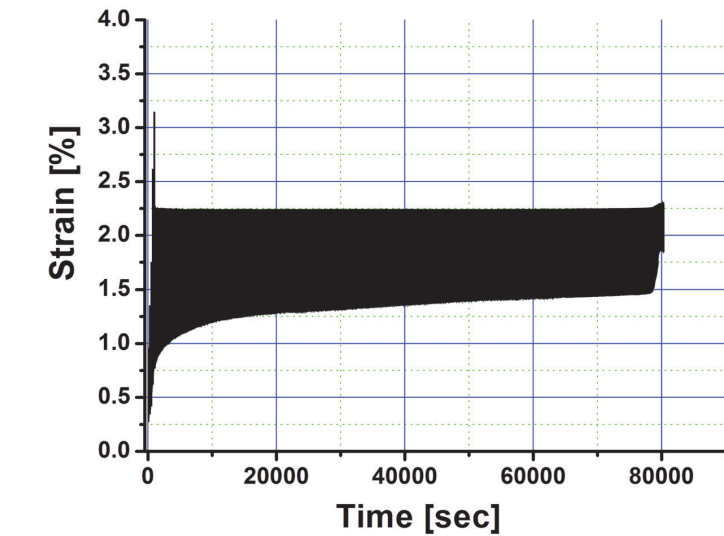


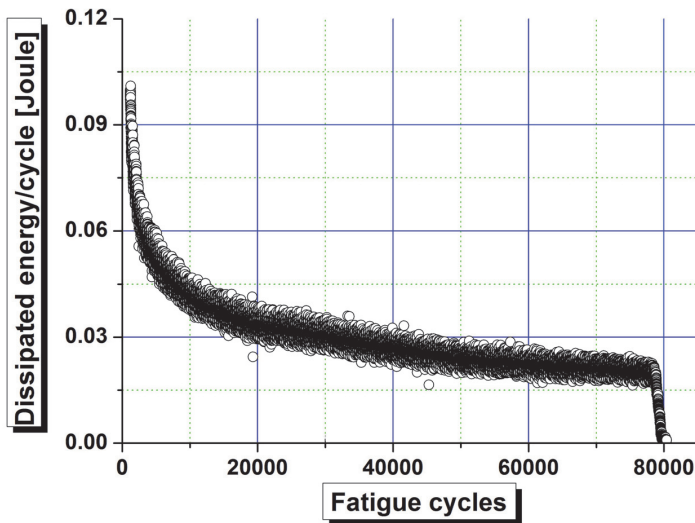
Figure 5: Fatigue test with preliminary mechanical treatment and then cycles up to 3.2% of strain and down to zero load. $\Theta = 25^{\circ}\text{C}$. Variability in time of the parameter η and of the elliptic cycle radius ηd .

In Figures 4a, 6a, and 8a, the progressively increasing trend of the minimum strain time history is in agreement with the corresponding plots in Figures 1b and it is due to the martensite retained in the specimen by microplasticity. Also the descendent trend of the maximum stress values which can be derived for test 3 from the force time history in Figure 8b is consistent with the one observed in Figure 1d and it is indicative of a decrease of the maximum transformation strain. It is worth noting that, also in Figure 8b, the target value of the unloading is set at different values to facilitate the identification of the two sets of cycles of different amplitude performed in each of the repeated sequences.

The time histories of the energy dissipated per cycle plotted in Figures 4b, 6b, and 9b show an overall descending trend which confirms the one observed in Figure 1c. Hence, the motivations discussed in the previous Section to justify such a behavior still hold. Nevertheless, the final branch corresponding to the loss of rigidity of the sample preceding its failure cannot be clearly identified in all Figures. This branch actually disappears in Figure 9b which refers to test 3, where the varying amplitude of the exciting cycles also leads to a significant scatter of the energy values along the entire time history. To provide further insight to this aspect, the



a)



b)

Figure 6: Fatigue test with preliminary mechanical treatment and then cycles up to 2.3% of strain and down to zero load. $\Theta = 25^{\circ}\text{C}$. a) full test with emphasis on the increasing of the residual strain; b) dissipated energy per cycle.

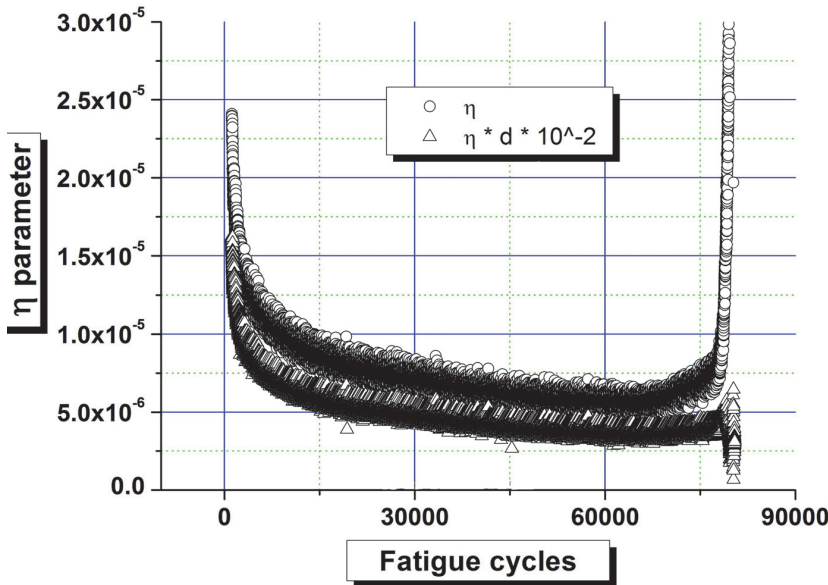
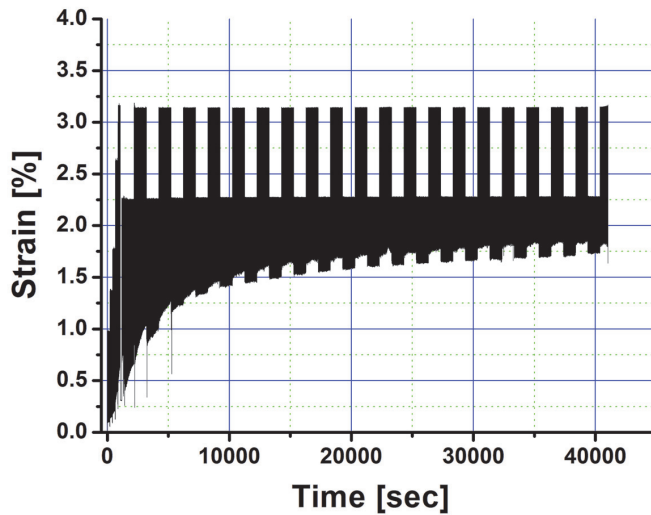


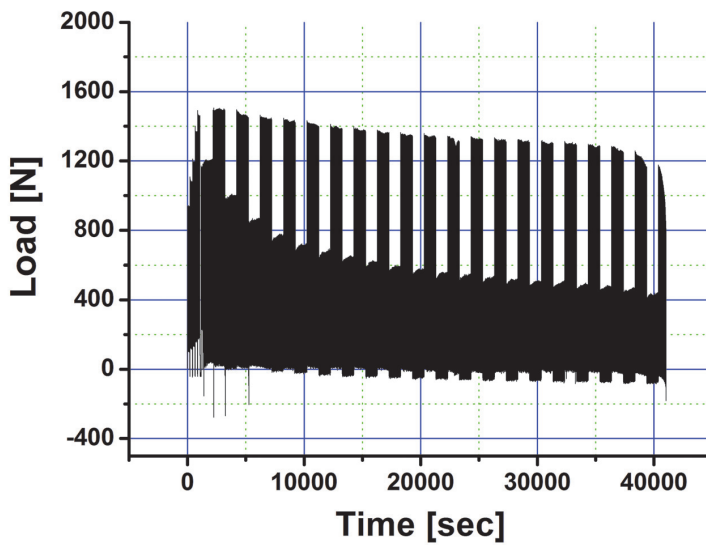
Figure 7: Fatigue test with preliminary mechanical treatment and then cycles up to 2.3% of strain and down to zero load. $\Theta = 25^{\circ}\text{C}$. Variability in time of the parameter η and of the elliptic cycle radius ηd .

data in Figures 8a and 8b are elaborated to represent, in Figure 9a, three couples of hysteresis cycles occurred at different times during the test. This latter plot not only outlines the trend of the minimum strain and the one of the maximum stress (visible also in Figure 8), but it also shows how the hysteresis loop (i.e., the amount of dissipated energy) evolves as the test proceeds. Since the loading is carried out in span control, i.e., up to the fixed maximum strain, the deterioration phenomenon is mainly expressed by an increase of the minimum strain and a decrease of the maximum stress; as a result, the area within the hysteresis loop can only decrease.

The inadequateness of the energy dissipated per cycle to detect the approaching of failure shifts the attention to the role of either the dimensionless parameter η given in Eq.(4), or equivalently to the shortest radius ηd of the ellipse approximating the hysteresis loop in the stress-strain plane, where d is defined in Eq.(3). The corresponding time histories are plotted together in Figure 5 for test 1 and in Figure 7 for test 2. In both cases, their root mean square values can be interpolated by a function with a negative first derivative until a stationary point is reached. This minimum point is located not far away from the failure situation and, therefore, it

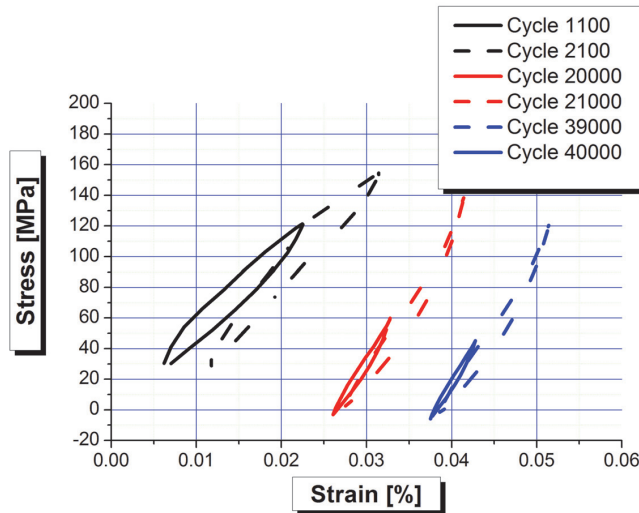


a)

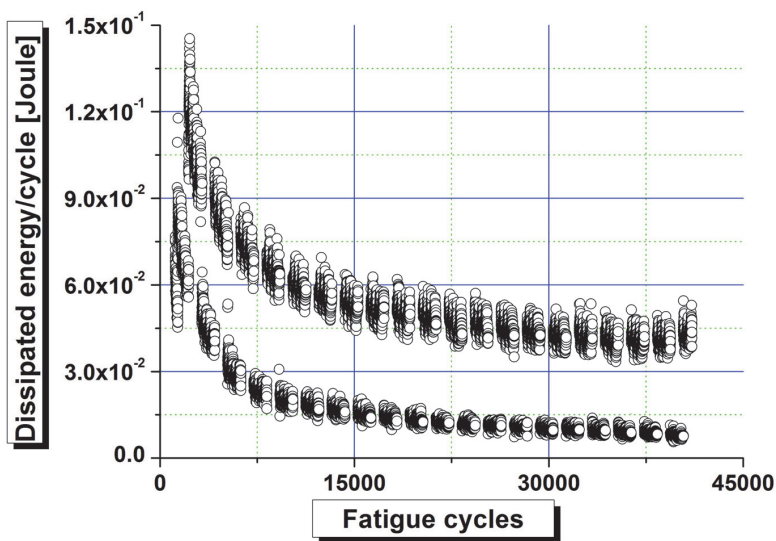


b)

Figure 8: Fatigue test with preliminary mechanical treatment: 1000 cycles up to 2.3% of strain and down to zero load, followed by 1000 cycles up to 3.2% of strain and down to zero load and so on. $\Theta = 25^{\circ}\text{C}$. a) strain time history, and b) load time history.

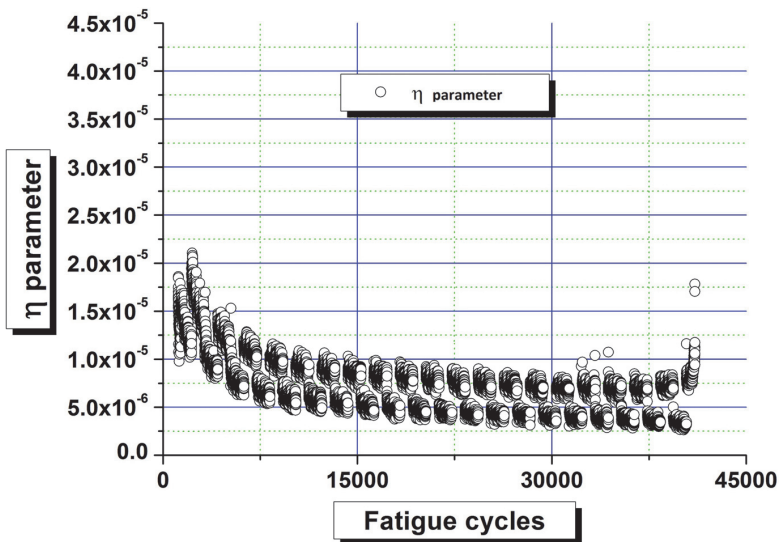


a)

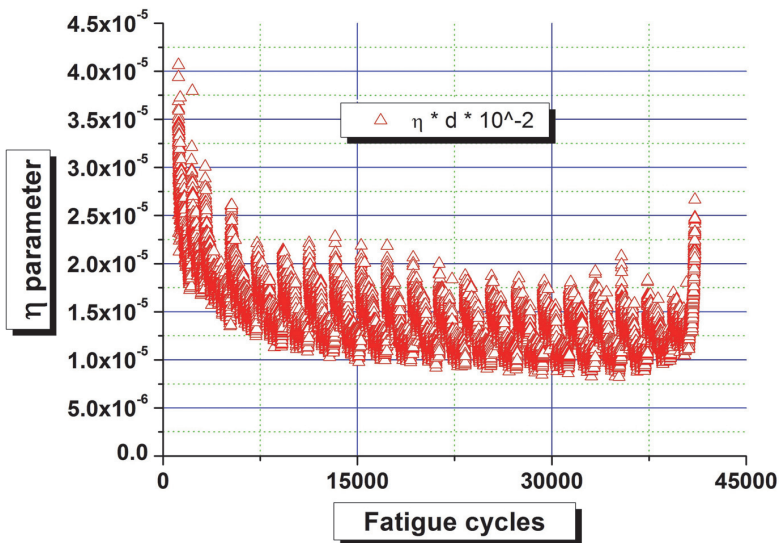


b)

Figure 9: Fatigue test with preliminary mechanical treatment and then 1000 cycles up to 2.3% of strain and down to zero load followed by 1000 cycles up to 3.2% and so on. The temperature is $\Theta = 25^{\circ}\text{C}$. In a) couples of stress-strain cycles are drawn: the shifts between the third couple and the previous couples are 0.02 and 0.01, respectively. In b) the energy per cycle sequence is reported.



a)



b)

Figure 10: Fatigue test with preliminary mechanical treatment and then 1000 cycles up to 2.3% of strain and down to zero load followed by 1000 cycles up to 3.2% and so on. The temperature is $\Theta = 25^\circ\text{C}$. Variability in time of the parameter η and of the elliptic cycle radius ηd

can be regarded as an alert of the loss of rigidity of the specimen.

For test 3, the time histories of the two quantities η and ηd are plotted separately in Figures 10a and 10b. The trend of the function interpolating their root mean square values is consistent to the one observed during tests 1 and 2. Therefore, the stationary point is regarded, also in this case, as an early alert of failure.

5 Modeling the damage accumulation

Standard damage accumulation models are governed by the so-called Miner's rule:

$$D = n_1/n_{c1} + \dots + n_N/n_{cN} \leq D_L \quad (7)$$

where D is a damage index and D_L is its threshold value. The damage index is built as the sum of N addenda, with N the number of different amplitudes occurred in a sequence of cycles. These addenda are the ratio between the number of cycles n_j , $j=1,\dots,N$, characterized by the same amplitude along the sequence and the number of cycles to rupture, n_{cj} , $j=1,\dots,N$, recorded during a fatigue test at that given intensity. It is assumed that $n_j < n_{cj}, \forall j$, so that each single addendum is lower than 1.

From the three tests discussed in the previous Section, the following assignments are made: $N=2$, $n_1=20000$ (i.e., 20 sets of 1000 cycles at lower intensity survived in test 3, as shown in Figure 8), $n_2=19654$ (i.e., 19 sets of 1000 cycles at upper intensity, plus further 654 cycles at the same intensity survived in test 3, as shown in Figure 8), $n_{c1}=80413$ (i.e., cycles at lower intensity survived in test 2, as shown in Figure 6), and $n_{c2}=32620$ (i.e., cycles at upper intensity survived in test 1, as shown in Figure 4). By substituting these values in Eq (7), the following estimate of the damage index is obtained:

$$D = 20000/80413 + 19654/32620 = 0.2487 + 0.6025 = 0.8512 = D_L \quad (8)$$

which coincides with its threshold value because test 3 ends with the rupture of the specimen.

As stated in [Augusti et al., 1984], "if Miner's rule is applied, the experimental failure most likely occurs with $D < 1$ ". Actually, the expected damage at failure is estimated to be triggered by $D = 0.83$ and this value is in perfect agreement with the result calculated above. This enables the authors to claim that the original (linear) Miner's rule can be adopted to accumulate the damage, despite the untraditional manner in which the cycles are carried out in the tests of Section 4. Indeed, although standard fatigue tests are driven in load control, the results in Section 4 are obtained by using span control during the loading and load control during the unloading, as suggested by the reasoning in Section 1.

Nevertheless, the application of the Miner's rule requires the knowledge of all the denominators, i.e., to carry out as many fatigue experiments at fixed amplitude as the number of different amplitudes present in the actual loading/unloading process. For this reason, the authors studied the feasibility of an alternative approach, which is based on the assessment of the dimensionless parameter η in Eq.(4), or even better its product by the quantity d in Eq. (5). In particular, one assumes that, in practice, the replacement of a structural element undergoing fatigue should take place after a number of cycles corresponding to the stationary point of the function interpolating the root mean square values of these quantities, which are computed based on continuously monitored strain gauges and load cell measurements. In other words, the observation of a change in the sign of the first derivatives of such functions is used as trigger for replacement in the maintenance policy, so that a satisfactory percentage of the actual fatigue lifetime of the structural element is exploited. To provide an example, this percentage is assessed using the data from Figures 5, 7 and 9. Let M the number of cycles up to rupture and M' the number of cycles up to the stationarity point; then the following estimates are obtained:

- cycles up to 3.2% of strain (test 1): $M' = 28000$, $M = 32620$, $M'/M = 86\%$;
- cycles up to 2.3% of strain (test 2): $M' = 70000$, $M = 80413$, $M'/M = 87\%$;
- mixed sequences of two sets of 1000 cycles each (test 3): $M' = 35000$, $M = 39654$, $M'/M = 88\%$.

6 Conclusions

The fatigue tests on Cu-Al-Be alloy bars reported in this paper refer to non-single grain specimens. They are characterized by a superelastic behavior at positive temperatures. Nevertheless, a trend to produce martensite during a cyclic loading-unloading of the bars is observed. The martensite retained in the specimen by micro-plasticity results in residual strain at the end of each cycle. Thus, the fatigue effect, related to the classical damage observed in a wide range of metallic materials, comes with a loss of specific properties of SMA during cyclic loading, which include, together with the increase of the retained martensite volume fraction, also a decrease of the maximum transformation strain, a shift of the transformation temperatures, etc. An effort to illustrate these phenomena based on the data achieved from laboratory tests is performed. Furthermore, a first attempt of modeling the material deterioration is discussed in this paper. In particular, the validity of the classical damage accumulation rule is verified experimentally. Finally, the possibility of measuring the variation of a dimensionless parameter η associated with

the dissipated energy per cycle is proposed in order to identify an early alert of collapse.

Acknowledgement: The research activity summarized in this paper has been supported by Athenaeum research grants from the University of Pavia (FAR 2008) and Catania (PRA 2008).

References

Augusti G., Baratta A. and Casciati F. (1984): *Probabilistic Methods in Structural Engineering*, Chapman & Hall, London.

Bertacchini O. W., Lagoudas D. C., Patoor E. (2009): Thermomechanical transformation fatigue of TiNiCu SMA actuators under a corrosive environment – Part I: Experimental results, *International Journal of Fatigue*, 31, 10, 1571-1578,

Carreras G., Casciati F., Casciati S., Isalgue1 A., Marzi A., Torra V. (2011): Laboratory fatigue testing toward the design of SMA portico-braces, *Smart Structures and Systems*, 7, 1, 41-57.

Casciati F., Faravelli L. (2009): A passive control device with SMA components: from the prototype to the model, *Journal of Structural Control and Health Monitoring*, 16, 7-8, 751-765. DOI: 10.1002/stc.328.

Casciati F., Faravelli L., Isalgue A., Martorell F., Soul H., Torra V. (2008): SMA fatigue in civil engineering applications, *Advances in Sciences and Technology*, Trans Tech Publications, Switzerland, Vol. 59, 168-177.

Casciati F., Rossi R. (2006): Sensor Devices Exploiting Cu-based SMA Physical Properties. In: Alfredo Gumes (ed.) *Structural Health Monitoring 2006*, Lancaster, PA: Destech. 1095-1102.

Casciati F., van der Eijk C. (2008): Variability in mechanical properties and microstructure characterization of CuAlBe shape memory alloys for vibration mitigation. *Smart Structures and Systems*, 4, 2: 103-122.

Casciati S., Faravelli L. (2008): Structural components in shape memory alloy for localized energy dissipation. *Computer & Structures*, 86, 330-339.

Casciati S., Marzi A. (2010): Experimental Studies on the Fatigue Life of Shape Memory Alloy Bars, *Smart Structures and Systems*, 6, 1, 73-85 .

Casciati S., Marzi A. (2011): Fatigue tests on SMA bars in span control, *Engineering Structures*, 33, 1232-1239.

DesRoches, R. McCormick, J., and Delemont, M. A. (2004): Cyclical Properties of Superelastic Shape Memory Alloys, *ASCE Journal of Structural Engineering*, 130, 1: 38-46.

- Dolce M, Cardone D, Marnetto R.** (2000): Implementation and testing of passive control devices based on shape memory alloys. *Earthquake Engineering and Structural Dynamics*; 29:945–968.
- Faravelli L., Marzi A.** (2010): Coupling shape-memory alloy and embedded informatics toward a metallic self-healing material, *Smart Structures and Systems*, 6, 9
- Graesser E.J., Cozzarelli F.A.** (1991): Shape memory alloys as new material for aseismic isolation. *Journal of Engineering Mechanics (ASCE)*; 117:2590–2608.
- Ip KH.** (2000): Energy dissipation in shape memory alloy wires under cyclic bending. *Smart Materials and Structures*, 9,5:653–659.
- Meunier M.-A., Trochu F., Charbonnier P.** (1996): Modeling of thermomechanical fatigue behavior in shape memory alloys using dual kriging. *Materials & Design*, 17, 3, 133-139.
- Nemat-Nasser S., Guo W.** (2006): Superelastic and cyclic response of NiTi SMA at various strain rates and temperatures. *Mechanics of Materials*, 38, 5-6, 463-474.
- Roy D., Buravalla V., Mangalgi P. D., Allegavi S., Ramamurty U.** (2008): Mechanical characterization of NiTi SMA wires using a dynamic mechanical analyzer. *Materials Science and Engineering A*, 494, 1-2, 429-435.
- Saiidi, M., M. O'Brien, Zadeh, S.** (2009): Cyclic response of concrete bridge columns using superelastic nitinol and bendable concrete. *ACI Structural Journal*, 106, 1: 69-77.
- Siredey, N., Eberhardt, A.** (2000): Fatigue behavior of Cu-Al-Be shape memory single crystals. *Materials Science and Engineering A*, 290, 1-2, , 171 – 179.
- Siredey N., Hautcoeur A., Eberhardt A.** (2005): Lifetime of superelastic Cu–Al–Be single crystal wires under bending fatigue. *Materials Science and Engineering A*, 396, 1-2, 296-301.
- Zhang X.P., Liu H.Y., Yuan B., Zhang Y.P.** (2008): Superelasticity decay of porous NiTi shape memory alloys under cyclic strain-controlled fatigue conditions. *Materials Science and Engineering: A*, 481-482, 170-173.